Form factors of pseudoscalar mesons

Mikhail Gorchtein, Peng Guo, and Adam P. Szczepaniak

Form factors of pseudoscalar mesons

Mikhail Gorchtein[1], Peng Guo[1] and Adam P. Szczepaniak[1,2]

[1] [2]*Center For Exploration of Energy and Matter,*
Indiana University, Bloomington, IN 47408, USA.
[2] *Physics Department, Indiana University,*
Bloomington, IN 47405, USA.

We consider the transition, $(\gamma^*\pi^0(\eta,\eta') \to \gamma)$ and electromagnetic $(\gamma^*\pi^\pm \to \pi^\pm)$ form factors in a wide range of energy-momentum transfer, s. We employ dispersion relations to connect the time-like and space-like region. We discuss the role of resonances and QCD, partonic contributions. We find that the former give sizable contributions in the currently available range of s and for the latter we consider the role of reggeized fermion exchange.

I. INTRODUCTION

Electromagnetic form factors of hadrons provide a clean tool to study their internal structure. At the real photon point, gauge invariance guarantees that the form factor is normalized to the net charge of the hadron under consideration. All form factors were found to decrease with the virtuality of the photon, the fact that is interpreted as the evidence for a non-trivial internal structure of hadrons. At low virtualities, a successful description is based on the picture in which the photon couples to pions, the lightest hadronic degree of freedom. This picture includes hadronic resonances in the timelike region.

In this paper we examine the charged pion electromagnetic form factor $F_{2\pi}(s)$, defined by the matrix element

$$\langle \pi^+(p')\pi^-(p)|J_\mu|0\rangle = e(p'-p)_\mu F_{2\pi}(s), \quad (1)$$

and the transition from factors between a neutral pseudoscalar meson $P = \pi^0, \eta, \eta'$ and a real photon, $F_{P\gamma}(s)$ determined by,

$$\langle P(p')\gamma(\lambda,p)|J_\mu|0\rangle = ie^2\epsilon_{\mu\nu\alpha\beta}\epsilon^{*\nu}(\lambda)p'^\alpha p^\beta F_{P\gamma}(s). \quad (2)$$

Here J_μ is the electromagnetic current, $s = (p'+p)^2$ is the four-momentum transfer squared *i.e.* mass squared of the virtual photon with $s > 0 (s < 0)$ corresponding to the time-like (space-like) photons, respectively. Current conservation implies $F_{2\pi}(0) = 1$ and, in the chiral limit, axial anomaly determination of the $\pi^0 \to 2\gamma$ decay leads to the expectation $F_{\pi\gamma}(0) \approx 1/(4\pi^2 f_\pi) = 0.274$ GeV^{-1} with $f_\pi = 92.4$ MeV being the pion decay constant, which is in excellent agreement with the experimental value of $F_{\pi\gamma}^{exp}(0) \approx 0.267$ GeV^{-1}. The measured values for the normalization of the η, η' transition form factors are $F_{\eta\gamma}^{exp}(0) \approx 0.272$ GeV^{-1} and $F_{\eta'\gamma}^{exp}(0) \approx 0.341$ GeV^{-1}, respectively. These can also be analyzed within the chiral framework, however, due to the large η, η' masses and the $\eta - \eta'$ mixing such analyses are not as firm as in the case of the π^0 from factor.

At short distances quark/gluon interactions are asymptotically free, and a rigorous prediction of perturbative QCD (pQCD) is that at high energy or momentum transfer, $|s| \gg \mu^2$, these form factors are determined by hard scattering of the external photon with a small number of the QCD constituents [1–5]. The available data on the pion electromagnetic form factor ranges up to $|s| \lesssim 10$ GeV^2 [6–16] and is approximately a factor of two above the asymptotic pQCD prediction. A strikingly large discrepancy with the pQCD prediction is observed in the pion transition form factor recently measured by BaBar [17]. For momentum transfers as large as $-s \approx 40$ GeV^2 the measurement disagrees with pQCD not only in normalization but also in the overall s-dependence. While pQCD predicts $sF_{\pi\gamma}(s) \to 2f_\pi =$ const. as $|s| \to \infty$ [4, 5], the data suggest that the magnitude of $-sF_{\pi\gamma}(s)$ grows with $|s|$. On the other hand, BaBar collaboration also measured the η and η' transition form factors [18, 19] up to $-s \approx 40$ GeV^2 in the spacelike region and at $s \approx 112$ GeV^2 in the timelike region, and these two form factors seem to be consistent with the pQCD expectations. This situation is often referred to as the "BaBar puzzle", in that from the pQCD prospective, it is unclear how the pion and the eta can exhibit such a different behavior.

One concludes that in the currently available range of energy or momentum transfers non-perturbative mechanisms must play an important role. In this paper we discuss a parametrization of such effects which is based on s-channel unitarity. For large, positive s, inelastic channel contributions play a similar role to the wee partons in the Feynman mechanism [20] for spacelike photons. Possible matching with pQCD is not addressed here, but we refer to [21] for discussion of this issue.

For moderate values of photon virtuality it is also necessary to consider contributions from resonances. Crossing symmetry implies that form factors are the boundary values of an analytic function defined in the complex-s plane with a unitarity cut running over the positive s-axis from the two pion production threshold branch

point $s_{th} = 4m_\pi^2$. Thus, to relate space-like and time-like region, it is natural to use dispersion relations (DR). In the time-like region the electromagnetic (transition) form factor describes the amplitude for production of a spin-1, $\pi^+\pi^-$ pair $(\pi^0\gamma, \eta\gamma, \eta'\gamma)$ in the external electromagnetic field of the virtual photon. In the space-like region form factors are usually interpreted in terms of parton three-momentum distribution in a hadron (and/or photon). Analyticity demands these apparently distinct physical pictures to be smoothly connected. The dominant feature of the spin-1, $\pi^+\pi^-$ amplitude is the isovector $\rho(770)$ resonance that also dominates the electromagnetic form factor. The pion transition form factor in the time-like region is sensitive to both ρ, and the isoscalar, $\omega(782)$ resonance. Analytical continuation to the space-like region implies that for $-s \lesssim 1\text{GeV}^2$, *i.e.* in the hadronic range, the quark wave function is dual to the vector-meson exchange in the crossed channel.

The paper is organized as follows. In the following section we relate the space-like and time-like regions through dispersion relations, discuss the resonance contribution and specifics of the model for the wee parton contribution. We give explicit formulas for the pion form factors. For the η and η' form factors analogous expressions can be derived and we only discuss those when presenting the numerical results. Summary and outlook is given in Section III

II. PION FORM FACTORS FROM DISPERSION RELATIONS

A. Resonance contribution

We begin with the discussion of the pion transition form factor $F_{\pi\gamma}(s)$. Its discontinuity across the unitary cut is given by

$$\text{Im}F_{\pi\gamma} = t^*_{2\pi,\pi\gamma}\rho_{2\pi}F_{2\pi} + t^*_{3\pi,\pi\gamma}\rho_{3\pi}F_{3\pi} + \sum_X t^*_{X,\pi\gamma}\rho_X F_X \tag{3}$$

and is illustrated in Fig. 1. In the last term the sum runs over all possible intermediate states $X \neq 2\pi, 3\pi$. Here,
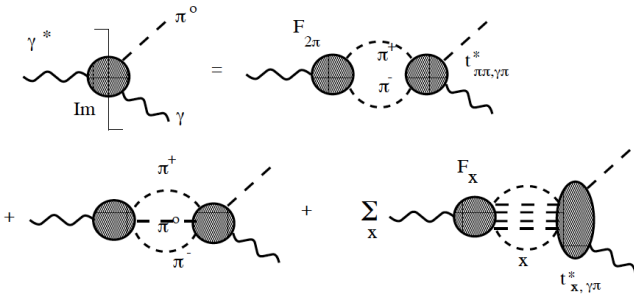

FIG. 1: Illustration of the various contributions to the discontinuity of the pion transition form factor, *cf* Eq. (3)

$t_{X,\pi\gamma}$ (F_X) represents the amplitude for $X \to \pi^0\gamma$ $(\gamma^* \to$

$X)$, respectively, whereas ρ_X represents the product of the phase space and kinematical factors, and for the 2π intermediate state it reads $(s_{th} = 4m_\pi^2)$

$$\rho_{2\pi}(s) = \frac{s(1 - s_{th}/s)^{3/2}}{96\pi}. \tag{4}$$

Provided that $\text{Im}F_{\pi\gamma}$ vanishes at $s \to \infty$, its real part can be reconstructed for any s from the unsubtracted dispersion relation,

$$F_{\pi\gamma}(s) = \frac{1}{\pi}\int_{s_{th}} ds' \frac{ImF_{\pi\gamma}(s')}{s'-s}. \tag{5}$$

The two lowest mass intermediate states, $X = 2\pi, 3\pi$ that are dominated by the $\rho(770)$ and $\omega(782)$ resonances, respectively, are expected to almost saturate the cut in the hadronic range $s_{th} < s \lesssim 1\text{GeV}^2$. The $\omega(782)$ in the isoscalar 3π channel is narrow, with the width to mass ratio,

$$\Gamma_\omega/m_\omega \sim 10^{-2} \tag{6}$$

and its contribution to $F_{\pi\gamma}$ can be well approximated by a Breit-Wigner distribution,

$$F_{\pi\gamma}^{(3\pi)}(s) = \frac{c_{\pi\gamma}^{(3\pi)}m_\omega^2}{[m_\omega^2 - s - im_\omega\Gamma_\omega(s)]}, \tag{7}$$

with

$$c_{\pi\gamma}^{(3\pi)} = \frac{g_{\omega\pi\gamma}}{m_\omega g_\omega} = 0.495F_{\pi\gamma}(0), \tag{8}$$

obtained from $\omega \to \pi\gamma$ and $\omega \to e^+e^-$ decay widths yielding $g_{\omega\pi\gamma} = 1.81$ and $g_\omega = 17.1$, respectively.

The contribution from the $\rho(770)$ to the 2π intermediate state determines both the $t_{2\pi,\pi\gamma}$ scattering amplitude and the pion electromagnetic form factor, $F_{2\pi}$ for $s \lesssim 1\text{GeV}^2$, and when represented in a form analogous to Eq. (7), yields

$$c_{\pi\gamma}^{(2\pi)} = \frac{g_{\rho\pi\gamma}}{m_\rho g_\rho} = 0.613F_{\pi\gamma}(0), \tag{9}$$

with $\rho \to \pi\gamma$ and $\rho \to e^+e^-$ decay widths leading to $g_{\rho\pi\gamma} = 0.647$ and $g_\rho = 4.96$. At $s = 0$ the sum of the ρ and ω resonance contributions to $F_{\pi\gamma}$ exceeds the measured value by 10-15%. The reason for this discrepancy is that the isovector contribution is broader than that of $\omega(782)$, and the effects of a finite width have to be taken into account properly. This can be achieved by using a unitary parametrization (*cf.* [22, 23]),

$$F_{2\pi}(s) = P(s)\Omega(s),$$
$$t_{2\pi,\pi\gamma}(s) = C^{-1}(s)\Omega(s). \tag{10}$$

Here $\Omega(s)$ is the Omnes-Muskelishvilli function [24, 25] that is computed from the phase of the vector-isovector

elastic $\pi\pi$ scattering amplitude. Close to the resonance position it resembles the Breit-Wigner form,

$$\Omega(s \sim m_\rho^2) \sim \frac{m_\rho^2}{m_\rho^2 - s - im_\rho\Gamma_\rho(s)}. \tag{11}$$

The polynomials $P(s)$ and $C(s)$ are determined from fits to the electromagnetic form factor and the solution to the DR for the $t_{2\pi,\pi\gamma}$ amplitude, respectively:

$$
\begin{aligned}
P(s) &= 1 + 0.1 s/m_\rho^2 \tag{12} \\
C(s) &= 4\pi^2 f_\pi^3 [1 + 1.27 s/m_\rho^2 + 1.38 s^2/m_\rho^4 - 0.50 s^3/m_\rho^6]
\end{aligned}
$$

In the energy range $1 \text{ GeV}^2 \lesssim s \lesssim \mu^2$, with $\mu^2 = 2 - 5$ GeV^2 being the upper mass range of resonance contributions to $K\bar{K}$ and other, few-hadron inelastic channels, are expected to contribute. For simplicity, in the following we ignore their contribution. Above the resonance region, $s \gtrsim \mu^2$, however, a possible determination of the multi-hadron contribution to the inelastic sum in Eq. (3) may be given in terms of the quark/gluon intermediate states, much like in the derivation of QCD sum rules (cf. [26]). Those will be discussed below in Sec. II B.

In the case of the pion electromagnetic form factor, the discontinuity across the unitary cut reads

$$\text{Im} F_{2\pi} = t^*_{2\pi,2\pi}\rho_{2\pi}F_{2\pi} + t^*_{K\bar{K},2\pi}\rho_{2K}F_K + \sum_X t^*_{X,2\pi}\rho_X F_X \tag{13}$$

where the sum is over the intermediate states X in $\gamma^* \to X \to 2\pi$ excluding $X = 2\pi, K\bar{K}$ which are included explicitly. Eq. 13 is illustrated in Fig. 2
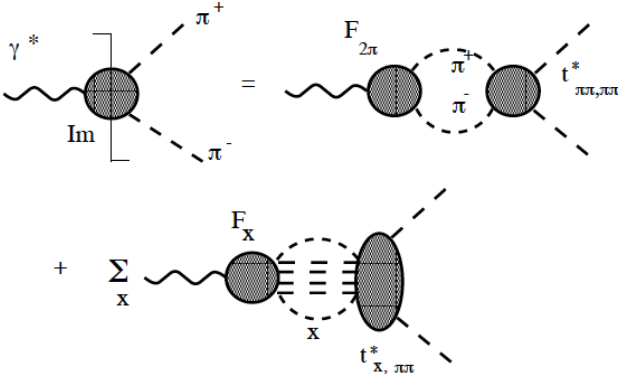

FIG. 2: Discontinuity of the pion electromagnetic form factor. The summation in the last diagram extends over all isovector, P-wave states except for the two pion state whose contribution is shown explicitly.

The two channels $X = 2\pi$ and $X = K\bar{K}$ are phenomenologically most significant in the hadronic domain [27]. The unitarity relation now involves both $\text{Im} F_{2\pi}$ and $\text{Re} F_{2\pi}$ (cf. the first term on the r.h.s of Eq. (13)) and above the inelastic threshold it can be solved algebraically [28]. Alternatively we can compute

$F_{2\pi}$ using Eq. (13) and the Cauchy representation. It is convenient to write the form factor in the form

$$F_{2\pi}(s) = N(s) / D(s) \tag{14}$$

with the numerator containing inelastic cuts. Then the dispersion relations for $N(s)$ and $D(s)$ follow from Eq. (13) and give, [28]

$$
\begin{aligned}
N(s) &= \sum_{X\neq 2\pi} \frac{1}{\pi} \int_{s_i} ds' \frac{D(s')Re\left[t^*_{X,2\pi}(s')\rho_X(s')F_X(s')\right]}{[1 - it^*_{2\pi,2\pi}(s')\rho_{2\pi}(s')](s'-s)} \\
D(s) &= \exp\left(-\frac{s}{\pi}\int_{s_{th}} ds' \frac{\phi(s')}{(s'-s)s'}\right), \tag{15}
\end{aligned}
$$

with the phase ϕ obtained from the elastic amplitude,

$$\tan\phi = \frac{\text{Re}t_{2\pi,2\pi}\rho_{2\pi}}{1 - \text{Im}t_{2\pi.2\pi}\rho_{2\pi}}. \tag{16}$$

As discussed earlier, the dominant feature of the pion electromagnetic form factor is the $\rho(770)$ resonance. Close to the resonance peak there is also a contribution from the isospin-violating $\omega \to 2\pi$ decay. Here we do not attempt to reproduce the details of the $\rho - \omega$ interference region. The next relevant feature is the large variation in magnitude of $|F_{2\pi}|$ at $\sqrt{s} \sim 1.7$ GeV which is also seen in the elastic $2\pi \to 2\pi$ amplitude and is attributed to the contribution from the inelastic $\rho''(1700)$ resonance decaying to $K\bar{K}$. We thus approximate the sum over inelastic channels in Eq. (15) by the single $K\bar{K}$ channel.

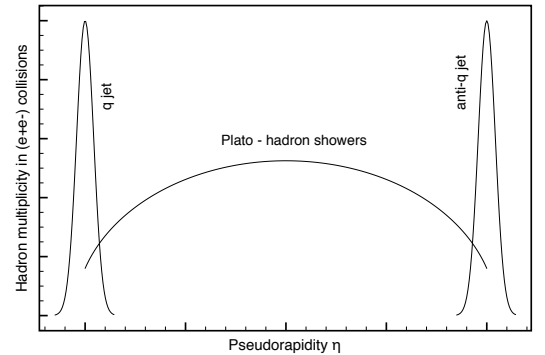### B. Multi-particle contribution

FIG. 3: Hadron multiplicity vs. pseudorapidity in e^+e^- collisions in arbitrary units.

In a high energy e^+e^- collision, a highly virtual time-like photon converts into a quark and an antiquark that travel in the opposite directions (in the rest frame of the virtual photon). These highly energetic quarks radiate gluons. If the leading mechanism is an emission of a small number of gluons, as expected in pQCD, with hard
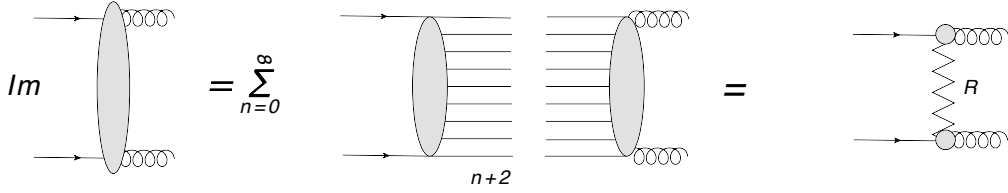
FIG. 4: The appearance of the reggized quark propagator (shown in the right diagram of Fig. 5) is illustrated on the example of the process $q\bar{q} \to gg$. Regge behavior comes about as a result of a resummation of an infinite ladder, $q\bar{q} \to q\bar{q} + n \to gg$ with n extra gluons or quarks and antiquarks in the intermediate state.

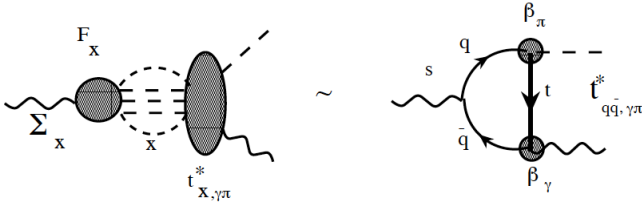FIG. 5: Sum over multi-particle intermediate states (left diagram) is represented by the $q\bar{q} \to \pi\gamma$ (right diagram), or $q\bar{q} \to \pi\pi$ in the case of electromagnetic form factor, amplitude which at high energies $s \to \infty$ is given by a Regge limit of a fermion (spectator quark) exchange.

gluon emission being power-suppressed, multi-particle production would result from a fire-ball decay of jets producing a broadening of the peaks around the initial q or $\bar{q}$ jet in the rapidity distribution, as shown in Fig. 3. To obtain the mid-rapidity plato that is observed in experiments, one needs to radiate a large number of gluons and $q\bar{q}$-pairs that neutralize color between the opposite side jets. They form hadron showers that fill in the mid rapidity region in Fig. 3. To account for this mechanism we recall that in QCD it was shown that multi-particle production corresponds to ladder exchanges. In particular for $q\bar{q} \to gg$ scattering these lead to an *effective* $q\bar{q} \to gg$ amplitude with a Reggeized quark exchanged in the t-channel [29–39], as illustrated in Fig. 4.

In the following, we will estimate the contribution of this mid-rapidity plato to the unitarity relations of Eqs. (3), (13) for the electromagnetic and transition form factors. Since the electromagnetic form factor F_X of a composite state decreases with energy-momentum transfer, asymptotically the highly virtual photon will couple to a single quark-antiquark pair. Thus, the contribution of interest to the *r.h.s* of Eqs. (3), (13) is given by the $X = q\bar{q}$, quark-antiquark intermediate state. Its form factor is $F_{q\bar{q}} = 1$ (in units of the quark charge) and the $q\bar{q}$ state contributes to $\mathrm{Im}F_{\pi\gamma}$ via the $q\bar{q} \to \pi\gamma$, P-wave scattering amplitude, $t_{q\bar{q},\pi\gamma}$ as illustrated in Fig. 5. For the electromagnetic form factor, instead of $t_{q\bar{q},\pi\gamma}$ the amplitude $t_{q\bar{q},\pi\pi}$ enters.

In the kinematically relevant domain $s \gg t \sim b^{-1}$, t

being the momentum squared carried by the exchanged quark and $b \approx$ few GeV^{-2} the typical slope of the product of residues of the exchanged quark $(\beta_\pi, \beta_\gamma)$, the amplitude $t_{q\bar{q},\pi\gamma}$ is expected to have a Regge behavior

$$t_{q\bar{q},\pi\gamma}(s,t) = \beta_\pi(t)\beta_\gamma(t)s^{\alpha_q(t)} \approx \beta_{\pi\gamma}e^{bt}s^{\alpha_q}. \quad (17)$$

The $q\bar{q}$ contribution shown in Fig. 5 may be contrasted with the one which represents the asymptotic contribution in the leading twist pQCD. In the latter, the $q\bar{q} \to \pi\gamma$ scattering amplitude, shown by the vertical line in the diagram on the right in Fig. 5, is given by a free quark propagator exchanged between the final state pion and photon. The difference between the free and the Regge propagator represents the multi-parton production which grows proportional to $\ln s$ and builds up the ladder shown in Fig. 4 (the cut in s of the ladder in Fig. 4 is the multi-particle amplitude).

However, just like the BFKL ladder model represents only a part of the Pomeron, the ladder shown in Fig. 4 may give only a partial contribution to the quark Regge trajectory $\alpha_q(t) \approx \alpha_q(0) + \alpha'_q t$. Thus, in the following we choose to employ a phenomenological approach and use the phenomenological relation between the quark trajectory and that of the leading Regge exchange in $\pi\pi$ scattering, *i.e.* the ρ or f_2 exchange that are nearly degenerate, *cf.* [40], $\alpha_\rho(t) \approx \alpha_{f_2}(t)$. Identifying reggeized ρ and f_2-exchanges with reggeized $q\bar{q}$-exchanges, leads to [41]

$$\alpha_q(t) \sim \frac{\alpha_\rho(t)}{2} + \frac{1}{2} \approx 0.75 + 0.45\frac{t}{GeV^2}. \quad (18)$$

It is worth noting that the dominance of quark-exchange (or, more precisely, quark *interchange*) mechanism has previously been observed in hard scattering processes with hadrons [42]. The hard scattering data are compatible with $\alpha_q(t = -1\,\mathrm{GeV}^2) \approx 0.3 - 0.4$ [43], which is consistent with Eq. (18). After projecting onto spin-1 partial wave (we refer the reader to Appendix for greater detail), the energy dependence of the asymptotic, $q\bar{q}$ contribution to $\mathrm{Im}F_{\pi\gamma}$ is therefore predicted to behave as (modulo terms $\sim O(\ln s)$),

$$s\mathrm{Im}F_{\pi\gamma}^{(q\bar{q})}(s) \to c_{\pi\gamma}^{(q\bar{q})}(s/GeV^2)^{\alpha_q(0)-1/2}. \quad (19)$$

The important point is that as long as $\alpha_q(0) > 1/2$, as implied by Eq. (18), the form factor, $sF_{\pi\gamma}(s)$ will increase with energy in agreement with the BaBar measurement.

C. Results

Combining the resonance contributions of Eqs. (7),(10) with the asymptotic form of Eq. (19) starting at $s > \mu^2$, we fit the the available pion transition form factor data using Eq. (5) with the single free parameter $c_{\pi\gamma}^{(q\bar{q})}$ (for several values of μ) as shown in Fig. 6. Our results for
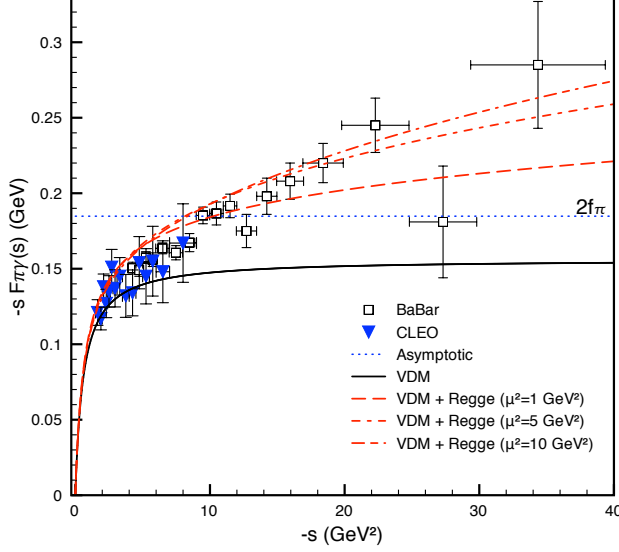

FIG. 6: (Color online) Our results for $|sF_{\pi\gamma}(s)|$ in the space-like region for $\mu^2 = 1$ GeV^2 (dashed red line), 5 GeV^2 (dash-dotted red line), 10 GeV^2 (double-dash-dotted red line), are confronted with the experimental data from [17, 46]. The hadronic (unitarized VDM) contribution is shown separately (solid black line). For comparison, the asymptotic limit $|sF_{\pi\gamma}^{as}(s)| = 2f_\pi$ is shown (blue dotted line).

the pion transition form factor are shown in Fig. 6. It is worth noting that even at largest values of $-s$ the bare $q\bar{q}$ production gives only about 50% (dash-dotted line in Fig. 6) of the form factor with the remaining half coming from the resonances. In Fig. 7, we show our results for the electromagnetic pion form factor F_π in the range -40 GeV$^2 \leq s \leq 10$ GeV^2. We confront them with the available experimental data for the electromagnetic form factor for -10 GeV$^2 \leq s \leq 10$ GeV^2 and the transition form factor for -40 GeV$^2 \leq s \leq -0.8$ GeV^2 (both are normalized to 1 at $s = 0$). First, we note that in the space-like region the data for the two form factors looks identical.

One can see that our model describes all the available data throughout the shown kinematics. There might be an indication of a resonance missing in our calculation in the region 2 GeV$^2 \lesssim s \lesssim 3$ GeV^2, probably coupled to the $K\bar{K}$ state. However, due to large error bars of the data its impact on the overall quality of the fit is expected to be negligible. This serves as an evidence that the s-dependence is in both cases driven by the same mechanism. In the case of the electromagnetic form factor,
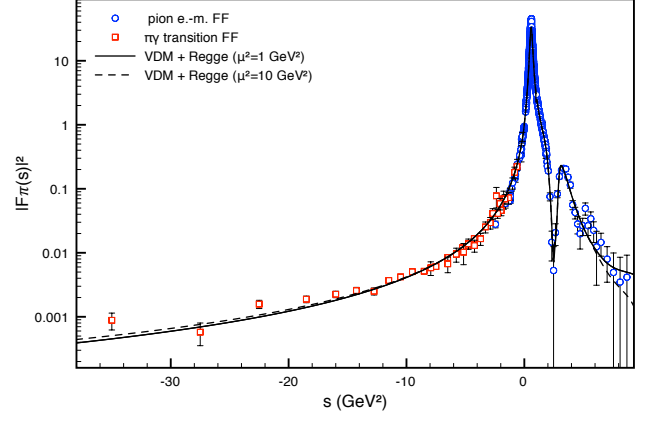

FIG. 7: (Color online) Our results for the pion electromagnetic form factor for $\mu^2 = 1$ GeV^2 (solid line) and $\mu^2 = 10$ GeV^2 (dashed line) vs. experimental data on the time-like and space-like e.-m. form factor from [6–16] (blue circles). Red squares show the pion transition form factor data from [17, 46] normalized to $F_{\pi\gamma}(0) = 1$.

our result is a prediction for the s-dependence at large $|s|$, where no data exist so far. In particular, we predict that, as for the transition form factor case, $|sF_{2\pi}(s)|$ has to rise asymptotically roughly as $s^{1/4}$, unless the mechanisms discussed here become reduced by Sudakov form factors and pQCD asymptotics takes over.

Recently, the BaBar collaboration also released data on transition form factors of η and η' [18]. Unlike the pion transition form factor these seem to have less pronounced rise with $|s|$. In Fig. 8 we display our results for the η and η' transition form factors. We display the two contributions separately: the unitarized VDM (with $g_{\rho\eta\gamma} = 1.23$, $g_{\omega\eta\gamma} = 0.35$, $g_{\phi\eta\gamma} = 0.7$, $g_{\rho\eta'\gamma} = 1.05$, $g_{\omega\eta'\gamma} = 0.35$, $g_{\phi\eta'\gamma} = 0.72$ and the unitarization of the ρ contribution similar as for the $\pi^0\gamma$ form factor), and its sum with the Regge contribution. We turn on the discontinuity represented by the asymptotic contribution above $\mu_R^2 = 5$ GeV^2 and fit the only remaining free parameter: the normalization $\beta_{\eta(\eta')\gamma} = c_{\eta(\eta')\gamma}^{(q\bar{q})}$, cf. Eq. (19). A unified description of all three transition form factors is achieved with $c_{\pi\gamma}^{(q\bar{q})} : c_{\eta\gamma}^{(q\bar{q})} : c_{\eta'\gamma}^{(q\bar{q})} = 0.067 : 0.038 : 0.025$. Note that rather than the absolute size of the Regge contribution that is similar for π^0, η, η', it is its size relative to the hadronic contribution that determines the s-dependence of the respective transition form factor. In fact, we observe that at $s = -40$ GeV^2 the hadronic contributions scale as $-sF_{P\gamma}^{had}(s) \approx 0.13\,(0.16, 0.21)$ for $P = \pi^0(\eta, \eta')$, respectively.

To better understand the origin of these numerical results, we recall that η and η' can be represented as a mixture of the isoscalar and strange states [47, 48],

$$|\eta\rangle = \cos\phi|I=0\rangle - \sin\phi|s\bar{s}\rangle$$
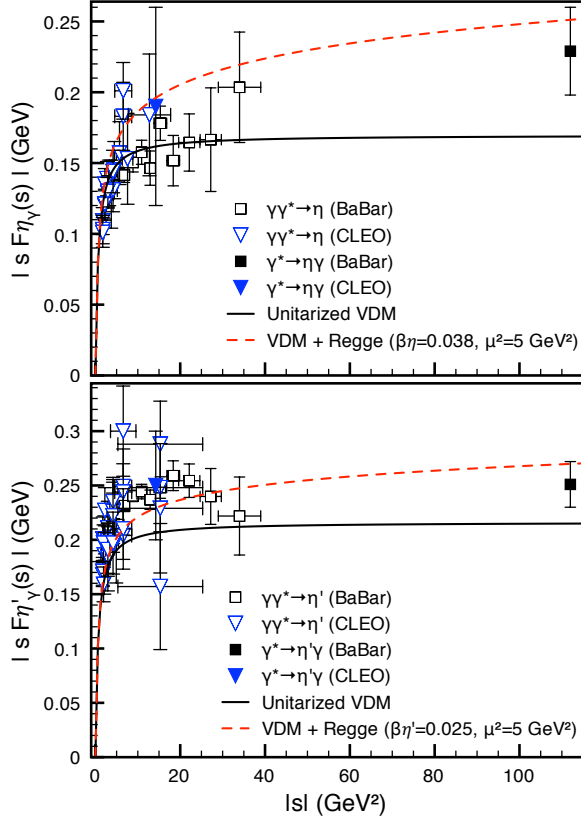$$|\eta'\rangle = \sin\phi|I=0\rangle + \cos\phi|s\bar{s}\rangle, \qquad (20)$$

FIG. 8: (Color online) Top panel: experimental data for $|sF_{\eta\gamma}(s)|$ in the space-like region from Refs. [18, 46] and high-s time-like data from Refs. [19] in comparison with unitarized VDM (solid line) and our full model (VDM + Regge) with $\mu^2 = 5$ GeV^2 (dashed line). Bottom panel: the same for $|sF_{\eta'\gamma}(s)|$.

with the mixing angle $\phi = \theta + \arctan\sqrt{2}$ and the isoscalar state $|I = 0\rangle = \frac{1}{\sqrt{2}}\{u\bar{u} + d\bar{d}\}$. The octet-singlet mixing angle θ varies, depending on the analysis, from $-20°$, see e.g. Ref. [47], to $-13°$ [48], thus $34° \lesssim \phi \lesssim 41°$. $SU(3)$ octet and singlet states are defined as $|8\rangle = \frac{1}{\sqrt{6}}\{u\bar{u} + d\bar{d} - 2s\bar{s}\}$ and $|0\rangle = \frac{1}{\sqrt{3}}\{u\bar{u} + d\bar{d} + s\bar{s}\}$, respectively. Also the octet and singlet states decay constants will in general differ from the purely isovector π^0 [47],

$$f_8 \approx 1.30 f_\pi$$
$$f_0 \approx 1.04 f_\pi. \tag{21}$$

Finally, in the calculation of the triangle graph, isoscalar combination of the quark charges instead of the isovector leads to a relative factor of $\frac{5}{3}$ with respect to the π^0 case. Using Eq. (B2) from the Appendix, Eqs.(20,21) and $\phi = 41°$, and neglecting the strange quarks contribution (we expect the s-quark to have a lower Regge intercept and to be subleading asymptotically), we obtain

the following estimate:

$$\frac{\mathrm{Im}F_{\eta\gamma}(s)}{\mathrm{Im}F_{\pi\gamma}(s)} \sim 1.03 \frac{\tilde{b}_{\pi\gamma}^2}{\tilde{b}_{\eta\gamma}^2}$$

$$\frac{\mathrm{Im}F_{\eta'\gamma}(s)}{\mathrm{Im}F_{\pi\gamma}(s)} \sim 1.16 \frac{\tilde{b}_{\pi\gamma}^2}{\tilde{b}_{\eta'\gamma}^2}, \tag{22}$$

where $\tilde{b}_{P\gamma} = b_{P\gamma} + \alpha'_q \ln(s/s_0)$ for $P = \pi^0, \eta, \eta'$, with $b_{P\gamma}$ the t-slope of the Regge residue in the $q\bar{q} \to P\gamma$ reaction, and α'_q the slope of the u, d-quark Regge trajectory. It can be seen that for moderate s (that is when $b_{P\gamma}$ terms dominate, see Eq.(A6) in the Appendix) the ratios can correspond to the fit values

$$c_{\pi\gamma}^{(q\bar{q})} : c_{\eta\gamma}^{(q\bar{q})} : c_{\eta'\gamma}^{(q\bar{q})} = 0.067 : 0.038 : 0.025 \quad \text{for}$$
$$b_{\pi\gamma} : b_{\eta\gamma} : b_{\eta'\gamma} = 1 : 1.35 : 1.76. \tag{23}$$

These parameters can in principle be deduced from the t-dependence of $\gamma\gamma \to \pi\pi$ and $\gamma\gamma \to \pi^0\eta(\gamma\gamma \to \pi^0\eta')$ differential cross sections at high energies. We plan to investigate this question in an upcoming work.

III. SUMMARY

We presented a calculation of the electromagnetic and transition form factors of the pion, η and η'. We used dispersion relations to provide a unified description of the pion form factors in the time-like and space-like regions. In the hadronic energy range, we accounted for hadronic, resonance contribution in a fully unitarized manner. For asymptotic contributions, we stressed the role of reggeization of the quark exchange which enhances energy dependence. We relate the parameters of such an exchange to $\pi\pi$ scattering data and deduce that the quark-Regge intercept is approximately $\alpha_q(0) - 1/2 \sim 1/4$. Using this value as input for the asymptotic behavior of the pion form factors, we obtain for both $sF(s) \propto s^{1/4}$, in agreement with the recent BaBar data. We notice that when the transition form factor is renormalized so that $F_{\pi\gamma}(0) = 1$ its dependence on s in the space-like region is consistent with that of the electromagnetic form factor, as shown by the open circles in Fig. 7. We use the normalization of the Regge-behaved $t_{q\bar{q},2\pi}$ and $t_{q\bar{q},P\gamma}$ as the only free parameter, and are able to describe all available data on pion, η and η' form factors.

The effect of multi-particle intermediate state on exclusive amplitudes has been considered in the past in the context of exclusive, hadronic B-meson decays [49]. The authors of [49] have found that final state interactions, due to multi-particle exchanges are important. Our model is close in spirit to that one, except the final state interactions are included at the parton level.

An example of a model based on analytical structure of the pion transition form factor that describes the BaBar data is [51]. The authors postulate an infinite sum over
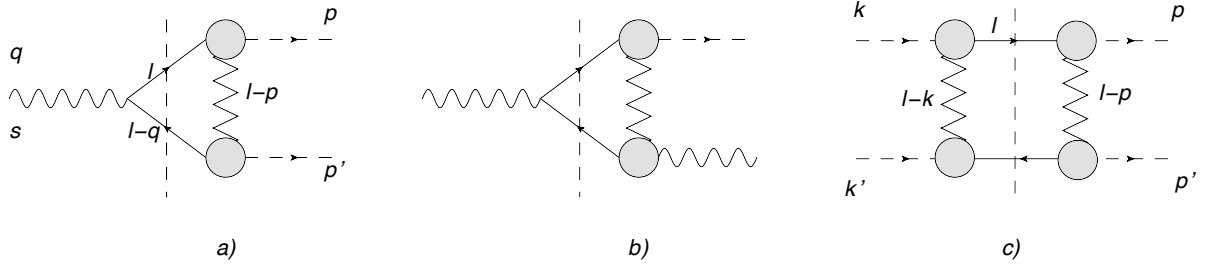
FIG. 9: Contributions of the reggeized quark exchanges to the imaginary parts of the pion electromagnetic form factor (diagram a), transition form factor (diagram b) and elastic $\pi\pi$-scattering (diagram c).

resonances in the s-channel of the $\gamma^* \to \gamma\pi^0$ process. Through Veneziano-like duality it leads to power-like Regge behavior of the transition form factor. We notice that both the model of Ref. [51] and ours obey the Terazawa-West bound [52, 53]. It is an intersting question, how that Veneziano-like approach is related to that of the present study: while Ref. [51] deals with duality and analyticity in terms of hadronic contributions, we address these properties at the level of quark subprocesses.

IV.   ACKNOWLEDGEMENTS

Appendix A: Asymptotics of the $q\bar{q} \to \pi\pi$-scattering amplitude with reggeized quark exchange from the elastic $\pi\pi$ amplitude

Here we consider the contribution of the reggeized quark exchanges as a model for the Reggeon (as opposed

to the Pomeron that is due to pure gluon exchanges) part of the asymptotic behavior of the meson-meson scattering amplitude. For the sake of simplicity and to avoid too many parameters that remain unconstrained, we will use the following form of the Regge propagator of the quark,

$$
\begin{aligned}
\mathcal{P}_R^{\pm}(s, t = q^2) &= P_R(s, t)(\slashed{q} \pm \sqrt{q^2}) \\
P_R(s, t) &= \pi \alpha_q' \left(\frac{s}{s_0}\right)^{\alpha_q(t)-\frac{1}{2}}.
\end{aligned}
\tag{A1}
$$

Here $\pm$ refers to the parity of the exchanged Reggeon (we refer the reader to [50] for a comprehensive discussion and details concerning fermion Regge exchanges). Note that the square root develops an imaginary part when taken in the s-channel scattering regime, $q^2 \le 0$; this square root has to be kept to ensure that the exchanged reggeized quark has a definite parity.

Correspondingly, we model the amplitudes for the processes $q\bar{q} \to \{\pi\pi; \pi\gamma; \gamma\gamma\}$ by the following Regge-behaved expressions:

$$
\begin{aligned}
T_{q(k)+\bar{q}(-k')\to\pi^a(p)+\pi^b(p')} &= \left(\frac{\beta_\pi}{2f_\pi}\right)^2 e^{b_{\pi\pi}t}\bar{v}(-k')\slashed{p}'\gamma_5\tau^b\mathcal{P}_R^{\pm}(s,t)\slashed{p}\gamma_5\tau^a u(k)\pi^a\pi^b \\
T_{q(k)+\bar{q}(-k')\to\pi^a(p)+\gamma(q')}^{\mu} &= iee_q\frac{\beta_\pi}{2f_\pi}e^{b_{\pi\gamma}t}\bar{v}(-k')\gamma^{\mu}\mathcal{P}_R^{\pm}(s,t)\slashed{p}\gamma_5\tau^a u(k)\pi^a \\
T_{q(k)+\bar{q}(-k')\to\gamma(p)+\gamma(q')}^{\mu\nu} &= -e^2e_q^2 e^{b_{\gamma\gamma}t}\bar{v}(-k')\gamma^{\mu}\mathcal{P}_R^{\pm}(s,t)\gamma^{\nu}u(k)
\end{aligned}
$$

The parameter β_π appearing above quantifies by how much the $q\pi q_R$ coupling differs from the pointlike chiral coupling $1/(2f_\pi)$, this latter corresponding to $\beta_\pi = 1$. Using Eqs. (A2,A1) (and massless quarks) we compute the imaginary part of the $\pi\pi$-scattering amplitude (*cf.* Fig. 9,c) from

$$
\begin{aligned}
\frac{1}{2i}[T_{\pi\pi}(s+i\epsilon,t) - T_{\pi\pi}(s-i\epsilon,t)] &= -N_c\frac{1}{2}\left[\frac{\beta_\pi}{2f_\pi}\right]^4\int\frac{d^4l}{(2\pi)^4}2\pi\delta(l^2)2\pi\delta((l-q)^2)P_R(s,t_2)P_R^*(s,t_1)e^{b_{\pi\pi}(t_1+t_2)} \\
&\times \mathrm{Tr}[(\slashed{l}+m_q)\slashed{p}\gamma_5(\slashed{l}-\slashed{p}\pm\sqrt{t_2})\slashed{p}'\gamma_5(\slashed{l}-\slashed{k}-\slashed{k}')(-\slashed{k}'\gamma_5)(\slashed{l}-\slashed{k}\mp\sqrt{t_1})(-\slashed{k}\gamma_5)],
\end{aligned}
\tag{A2}
$$

where we defined $t_1 = (l - k)^2$ and $t_2 = (l - p)^2$, $t = (k - p)^2$, $s = (k + k')^2 = (p + p')^2$, and $t_2 \approx t_1 + t + 2\sqrt{tt_1} \cos \phi$ for small negative t, t_1. The calculation of the trace in the above leads to $\mathrm{Tr}[\ldots] = st_1 t_2 (t_1 + t_2 - t) + 2t_1^2 t_2^2$, where only the first term contributes to the leading s behavior. Next, we change the variables $d \cos \theta_l \approx \frac{2}{s} dt_1$ (θ_l being the polar angle of the intermediate quark with the momentum l) and write

$$
\begin{aligned}
\mathrm{Im} T_{\pi\pi}(s, t) &= -\frac{N_c \beta_\pi^4 (\pi \alpha_q')^2}{256 \pi f_\pi^4} \left(\frac{s}{s_0}\right)^{2\alpha_q(0)-1} \int_{-s}^0 dt_1 \frac{1}{2\pi} \int_0^{2\pi} d\phi \, e^{(b_{\pi\pi} + \alpha_q' \ln \frac{s}{s_0})(t_1 + t_2)} t_1 t_2 (t_1 + t_2 - t) \\
&= \frac{3 N_c \beta_\pi^4 \pi \alpha_q'^2}{1024 f_\pi^4 \tilde{b}_{\pi\pi}^4} \left(\frac{s}{s_0}\right)^{2\alpha_q(0)-1} e^{\frac{2}{3} \tilde{b}_{\pi\pi} t},
\end{aligned} \tag{A3}
$$

where $\tilde{b}_{\pi\pi} = b_{\pi\pi} + \alpha_q' \ln \frac{s}{s_0}$. To arrive at the above result, the exact forward limit was calculated analytically; then, for $-t \leq 1 \, \mathrm{GeV}^2$ the integral was performed numerically and the resulting t-dependence was fitted by an exponential. This result should be confronted with the contribution of the (nearly degenerate) ρ, f_2 exchange to the $\pi\pi$ scattering amplitude (e.g., from Ref. [40])

$$
\mathrm{Im}_\rho T_{\pi\pi} = \beta_\rho \left(\frac{s}{s_0}\right)^{\alpha_\rho(t)} e^{B_\rho t} \tag{A4}
$$

with

$$
\begin{aligned}
\beta_\rho &= 1.02 \\
\alpha_\rho(t) &\approx 0.52 + 0.9t \\
B_\rho &\approx 2.4 \, \mathrm{GeV}^{-2} \tag{A5}
\end{aligned}
$$

We find good agreement for the following values of parameters:

$$
\begin{aligned}
\alpha_q(t) &= \frac{\alpha_\rho(t) + 1}{2} \approx 0.76 + 0.45t \\
b_{\pi\pi} &= 3.6 \, \mathrm{GeV}^{-2} \\
\beta_\pi &= 1.12 \tag{A6}
\end{aligned}
$$

The obtained values for $b_{\pi\pi}$ and β_π are very approximate, and are quoted here mostly to demonstrate that the fit returns reasonable values, i.e. $\beta_\pi \sim 1$, $b_{\pi\pi} \sim$ few GeV^{-2}. However, one should keep in mind that the values of Ref. [40] for the normalization β_ρ and the t-slope B_ρ bear a significant uncertainty. The main result of this Appendix is in the value of the quark Regge intercept $\alpha_q(t)$.

Appendix B: Asymptotics of the pion electromagnetic and transition form factors

For the pion electromagnetic form factor, Fig. 9, a) after the trace calculation we obtain,

$$
\begin{aligned}
\mathrm{Im} F_{2\pi}(s) &= \frac{N_c (e_u - e_d) \beta_\pi^2 \pi \alpha_q'}{16 \pi f_\pi^2 s_0} \int_{-s}^0 dt_2 \, e^{\tilde{b}_{\pi\pi} t_2} t_2^2 \left(\frac{s}{s_0}\right)^{\alpha_q(0)-\frac{3}{2}} \\
&= \frac{3 \beta_\pi^2 \alpha_q'}{8 f_\pi^2 s_0 \tilde{b}_{\pi\pi}^3} \left(\frac{s}{s_0}\right)^{\alpha_q(0)-\frac{3}{2}} \tag{B1}
\end{aligned}
$$

Similarly, for the pion transition form factor Fig. 9, b)

$$
\mathrm{Im} F_{\pi\gamma}(s) = -\frac{N_c (e_u^2 - e_d^2) \beta_\pi \pi \alpha_q'}{8\pi f_\pi s_0} \int_{-s}^0 dt_2 \, e^{\tilde{b}_{\pi\gamma} t_2} t_2 \left(\frac{s}{s_0}\right)^{\alpha_q(0)-\frac{3}{2}} = \frac{N_c \beta_\pi \alpha_q'}{24 f_\pi s_0 \tilde{b}_{\pi\gamma}^2} \left(\frac{s}{s_0}\right)^{\alpha_q(0)-\frac{3}{2}} \tag{B2}
$$

We next make use of Eq. (A3) rewritten in the form

$$
\sqrt{\mathrm{Im} T_{\pi\pi}(s, t = 0)} = \frac{3\sqrt{\pi} \beta_\pi^2 \alpha_q'}{32 f_\pi^2 \tilde{b}_{\pi\pi}^2} \left(\frac{s}{s_0}\right)^{\alpha_q(0)-\frac{1}{2}}, \tag{B3}
$$

$$
\begin{aligned}
\mathrm{Im} F_{2\pi}(s) &= \frac{4\sqrt{\mathrm{Im} T_{\pi\pi}(s, t = 0)}}{\sqrt{\pi} \tilde{b}_{\pi\pi} s} \\
\mathrm{Im} F_{\pi\gamma}(s) &= \frac{4 f_\pi \sqrt{\mathrm{Im} T_{\pi\pi}(s, t = 0)}}{3 \beta_\pi \sqrt{\pi} s} \tag{B4}
\end{aligned}
$$

to obtain our estimates for the asymptotic behavior of the pion form factors:

Using estimates for the numerical values of the parameters, obtained in the previous section, we predict the

asymptotic behavior of the pion form factors to be

$$\mathrm{Im}F_{2\pi}(s) \;\approx\; \frac{0.63}{1 + 0.125\ln(s/s_0)}\left(\frac{s}{s_0}\right)^{-\frac{3}{4}}$$

$$\mathrm{Im}F_{\pi\gamma}(s) \;\approx\; 0.067\left(\frac{s}{s_0}\right)^{-\frac{3}{4}}, \tag{B5}$$

where for simplicity we assumed that the Regge residue at the $q_R\gamma q$ vertex is equal to that at the $q\pi q$ vertex, $b_{\pi\gamma} \approx b_{\pi\pi}$. Note that this is a prediction that does not depend on the explicit value of the quark Regge trajectory intercept. This result was obtained by identifying the ρ exchange with the double quark-Regge exchange. In principle, one may hope to deduce the slope of that residue without such assumptions from the asymptotics of a photo-induced reaction, such as $\gamma\gamma \to \pi\pi$ or from light-by-light scattering. However, data for these reactions at high energies are not available, so we choose the assumption that the two slopes are similar for the time being.

[1] S. J. Brodsky, G. R. Farrar, Phys. Rev. Lett. **31**, 1153 (1973).
[2] A. V. Efremov and A. V. Radyushkin, Theor. Math. Phys. **42**, 97 (1980).
[3] A. Duncan, A.H. Mueller, Phys. Rev. D **21**, 1636 (1980).
[4] G.P. Lepage and S.J. Brodsky, Phys. Lett. B **87**, 359 (1979).
[5] G.P. Lepage and S.J. Brodsky, Phys. Rev. D **22**, 2157 (1980).
[6] C.N. Brown *et al.*, Phys. Rev. D**8**, 92 (1973).
[7] C.J. Bebek *et al.*, Phys. Rev. D**13**, 25 (1976).
[8] J. Volmer *et al.*, Phys. Rev. Lett. **86**, 1713 (2001).
[9] V.M. Aulchenko *et al.*, JETP Lett. **82**, 743 (2005).
[10] A. Aloisio, Phys. Lett. B**606** ,12 (2005).
[11] R.R. Akhmetshin *et al.*, JETP Lett. **84**, 413 (2006).
[12] M.N. Achasov *et al.*, J. Exp. Theor. Phys. **103**, 380 (2006).
[13] T. Horn *et al.*, Phys. Rev. Lett. **97**, 192001 (2006).
[14] V. Tadevosyan *et al.*, Phys. Rev. C**75**, 055205 (2007).
[15] R.R. Akhmetshin *et al.*, Phys. Lett. B **648**, 28 (2007).
[16] B. Aubert *et al.*, Phys. Rev. Lett. **103**, 231801 (2009).
[17] B. Aubert *et al.*, Phys. Rev. D **80**, 052002 (2009).
[18] B. Aubert *et al.*, [BABAR Collaboration] arXiv:1101.1142
[19] B. Aubert *et al.*[BABAR Collaboration], Phys. Rev. D **74**, 012002 (2006); T. K. Pedlar *et al.*[CLEO Collaboration], Phys. Rev. D **79**, 111101 (2009).
[20] R.P. Feynman, *Photon-Hadron Interactions*, (W.A.Benjamin Inc. NY, 1972).
[21] A. Efremov and A. Radyushkin, Mod. Phys. Lett. A **24**, 2803 (2009).
[22] T. N. Pham, T. N. Truong, Phys. Rev. D **14**, 185 (1976).
[23] T.N. Truong, Phys. Rev. D **65**, 056004 (2002).
[24] R. Omnes, N. Cim. **8**, 316 (1958),
[25] N. I. Muskhelishvili, Trud. Tbil. Mat. Inst. **10**, 1 (1958).
[26] B. L. Ioffe, A. V. Smilga, Phys. Lett. **114B**, 353 (1982).
[27] In Eq. (13) we use the following normalization for the elastic amplitude: $t_{2\pi,2\pi} = (\eta\exp(2i\delta) - 1)/2i\rho_{2\pi}$ where η and δ are the P-wave inelasticity and phase shift, respectively. The phase space factors, ρ_X are normalized accordingly and differ from those in Eq. (3), *i.e.* $\rho_{2\pi} = (1 - s_{th}/s)^{1/2}$.
[28] T. N. Pham, T. N. Truong, Phys. Rev. D **16**, 896 (1977).
[29] V. S. Fadin, V. E. Sherman, Sov. Phys. JETP **45**, 861 (1977).
[30] A. V. Bogdan, V. S. Fadin, Nucl. Phys. B **740**, 36 (2006).
[31] J. Kwiecinski, Phys. Rev. D **26**, 3293 (1982).
[32] L.N. Lipatov, M.I. Vyazovsky, Nucl. Phys. B **597**, 399 (2001).
[33] A. V. Bogdan, V. Del Duca, V. S. Fadin, E. W. Nigel Glover, JHEP **0203**, 032 (2002).
[34] M. I. Kotsky, L. N. Lipatov, A. Principe, M. I. Vyazovsky, Nucl. Phys. B **648**, 277 (2003).
[35] V. S. Fadin, M. G. Kozlov, A. V. Reznichenko, Phys. Atom. Nucl. **67**, 359 (2004).
[36] V. S. Fadin, M. G. Kozlov, A. V. Reznichenko Yad. Fiz. **67**, 377 (2004).
[37] A. V. Bogdan, V. S. Fadin, Nucl. Phys. B **740**, 36 (2006).
[38] V. S. Fadin, R. Fiore, M. G. Kozlov, A. V. Reznichenko, Phys. Lett. B **639**, 74 (2006).
[39] A. V. Bogdan, A. V. Grabovsky, Nucl. Phys. B **773**, 65 (2007).
[40] J.R. Peláez, F.J. Ynduráin, Phys. Rev. D **71**, 074016 (2005).
[41] Ya. Azimov, Zh. Eksp. i Teor. Fiz. **43**, 2321 (1962).
[42] C. White *et al.*, Phys. Rev. D **49**, 58 (1994).
[43] M. Strikman, Nucl. Phys. A **805**, 369 (2008).
[44] F. Felicetti, Y. Srivastava, Phys. Lett. B **107**, 227 (1981).
[45] P. Guo, R. Mitchell, A.P. Szczepaniak, Phys. Rev. D**82**, 094002 (2010).
[46] J. Gronberg *et al.*[CLEO Collaboration], Phys. Rev. D **57**, 33 (1998).
[47] E. P. Venugopal, B. R. Holstein, Phys. Rev. D**57**, 4397 (1998).
[48] C. E. Thomas, JHEP **10**, 026 (2007).
[49] J. F. Donoghue, E. Golowich, A. A. Petrov, J. M. Soares, Phys. Rev. Lett. **77**, 2178-2181 (1996).
[50] V. N. Gribov, Y. L. Dokshitzer, J. Nyiri, "Strong Interactions of Hadrons at High Energies: Gribov Lectures on Theoretical Physics", Cambridge Monographs on Particle Physics, Nuclear Physics and Cosmology, (2009).
[51] E. R. Arriola and W. Broniowski, Phys. Rev. D**81**, 094021 (2010).
[52] H. Terazawa, Phys. Rev. D**6**, 2530 (1972).
[53] G. B. West, Phys. Rev. Lett. **30**, 1271 (1973).